

201986: gold nugget, 47K Patch prospect (Sholl Terrane, northwest Pilbara Craton)

Sample type	Gold nugget
Total weight	3.6 g
Sample location	47K Patch, about 32 km south of Karratha
Coordinates	MGA Zone 50, 492217E 7676570N
Datum	GDA94
1:250 000 map sheet	YARRALLOOLA (SF 50-6)
1:100 000 map sheet	PINDERI HILLS (2255)
Tenement	E 47/3443; P 47/2039-S
Collector	Artemis Resources Limited



Location and sampling

The sample was provided by Artemis Resources Limited in January 2019. The gold nugget came from a colluvial/eluvial patch (compiled out of the GSWA 1: 100 000 scale geological series maps; GSWA, 2020) at the 47K Patch prospect in the northwest Pilbara region (Artemis Resources Limited, 2019, written comm., 11 January).

Geological context

The 47K Patch prospect is located about 6 km east of the Maitland Shear Zone, interpreted as a low angle thrust, in the Sholl greenstone belt of the Sholl Terrane in the northwest Pilbara Craton (Hickman, 2016; GSWA, 2020). The local bedrock includes metamorphosed pillow and massive basalt, dolerite sills, and minor felsic tuff, sandstone, shale, and chert of the 3117 – 3115 Ma Bradley Basalt. Metamorphosed massive hornblende monzogranite and syenogranite of the c. 2930 Ma Yannery Granite are exposed about 0.7 km east-southeast of the sample locality. Northeasterly striking Proterozoic dolerite dykes transect the area (Hickman, 2021, 2022; GSWA, 2020).

Artemis Resources Limited recovered around 6 kg (193 oz) of nuggety and fine-grained gold from colluvial–eluvial scree at the 47K Patch prospect in 2018, during shallow surface rehabilitation work. The gold is believed to have been shed from bedrock conglomerate-hosted mineralization (Artemis Resources Limited, 2018).

The nearest regolith landform — mapped by GSWA at the 1: 100 000 scale — is an alluvial–fluvial unit comprising unconsolidated gravel, sand, silt, and clay in active, but poorly defined drainage channels on floodplains (GSWA, 2020).

Methodology

The gold sample was photographed and weighed, and its overall morphology and external features, such as colour, roundness, surface relief, coatings, mineral inclusions, and mineral assemblages were recorded using

visual morphometry. The raw surface of the sample was analysed using scanning electron microscopy with energy dispersive X-ray system (SEM-EDS). The sample was then mounted in epoxy resin, cut and polished, and the gold grain microstructure, inclusions, and silver content were examined using reflected-light microscopy and SEM-EDS. Gold microchemistry was determined by laser ablation inductively coupled plasma mass spectrometry (LA-ICP-MS), calibrated against certified gold reference materials (CRM; Murray, 2009). The sample was ablated in triplicate along 0.5 mm-long traverses and average values calculated for elements present in the CRM. The gold surface was repolished after laser ablation, etched with aqua regia, and internal structure examined using reflected-light microscopy. The gold surface was repolished after etching, cleaned using ion beam milling, and its internal structure analysed using scanning electron microscopy with electron back-scattered diffraction (SEM-EBSD). Details of this method are described in Hancock and Beardsmore (2020).

Morphology

The gold nugget has dimensions of 10 x 9 x 5 mm, and a perfectly rounded and slightly flattened ('melon seed') shape, with a smooth, shiny, brown-orange surface containing patches of ferruginous quartz and Fe-oxide minerals (Fig. 1).

SEM-EDS analysis of raw surfaces

The overall orange-brown colour of the gold nugget surface arises from a fine film of Fe–Al clays, and darker brown patches consist of solid Fe-oxide minerals. There is no detectable Ag on the nugget surface.



Figure 1. Sample 201986: gold nugget, 47K Patch prospect

Optical microscopy of polished surfaces

In the polished section, about 50% of the sample surface is seen to consist of quartz, clays, and Fe-oxides minerals that fill what were once large voids and veinlets in the gold. Intergranular spaces between quartz grains, and pores in microplaty and reniform Fe-oxide minerals, are filled with clays and abundant disseminated gold nanoparticles (Fig. 2).

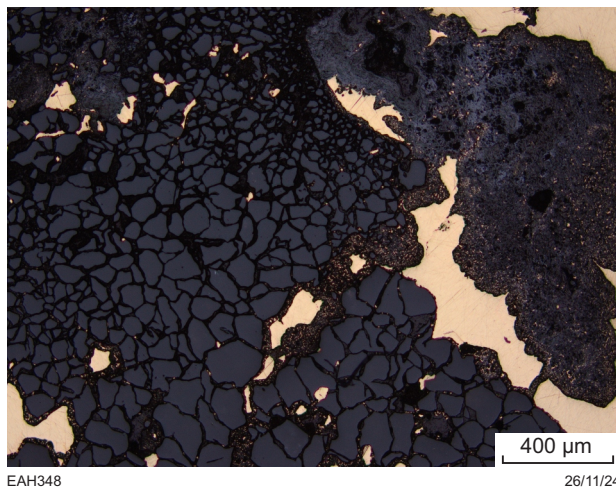


Figure 2. Reflected-light photomicrograph of polished surface of sample 201986: gold nugget, 47K Patch prospect

SEM-EDS analysis of polished surfaces

Coherent gold contains 7 % Ag. Margins between quartz and gold are encrusted by up to 100 µm rims of mixed clay and gold nanoparticles (Fig. 3a). Intergranular spaces between granulated quartz grains are filled by the same material. Gold crystal faces with columnar growth pattern were observed in a hole (probably once a bubble) in the gold polished surface (Fig. 3b).

LA-ICP-MS analysis

Ag, Cu and Hg were consistently detected within the gold grain, in concentrations higher than the instrument detection limit, and probably occur as limited solid solutions in the gold. The gold contains 7.1–8.5% Ag, and moderate amounts of Cu and Hg (583–651 ppm and 213–286 ppm respectively) (Table 1). Mg, Al, Ti, Ni, Zn, Nb, Cd, and Sn were also consistently detected in the gold at very low (in sub-ppm) concentrations (Table 2), possibly occurring in micro- and nano-inclusions. Elevated abundances of Ca and other lithophile elements detected in the ablation Traverses 1 and 2 suggest the presence of rock-forming mineral inclusions.

Acid etching

Gold in the sample occurs in several irregular masses with ragged dissolution margins. The internal microstructure of each mass comprises larger crystals having incoherent single twinning (Fig. 4a), abutting domains containing smaller, subangular to rounded gold grains with incoherent polysynthetic twin planes and curved and deformed grain boundaries. There are many intergranular veinlets filled with less Ag gold or with clay and gold nanoparticles (Fig. 4b). An outer rim of finer-grained, recrystallized gold is not obvious.

SEM-EBSD analyses

To confirm observations of the acid etched nugget surface and determine whether an outer rim of very fine-grained gold is indeed absent, the cut surface was further etched using ion beam milling and analysed using SEM-EBSD. This confirmed the recrystallized, polycrystalline microstructure of the coherent gold masses, their disaggregation from one another along former intergranular veinlets and dissolution of subgrain edges, and filling of resulting voids with regolith material (Fig. 5). There is also a very thin outer rim no greater than 50 µm wide comprising very fine-grained, recrystallized gold.

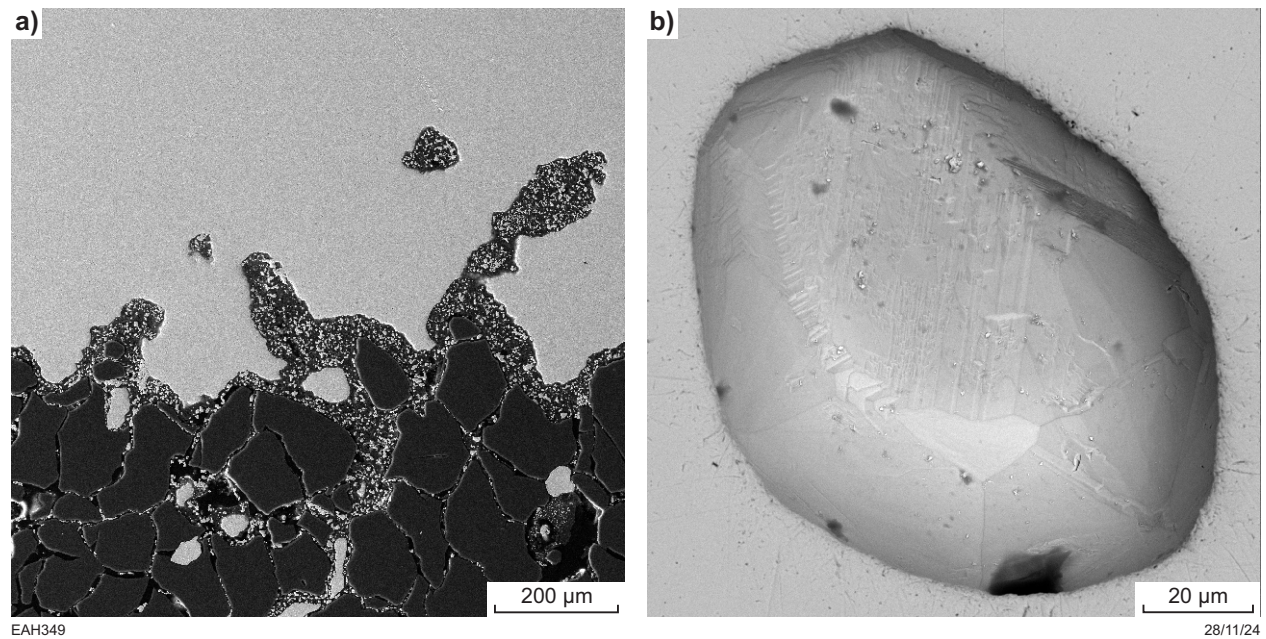


Figure 3. Backscattered electron and secondary electron images of polished surfaces of selected areas of sample 201986: gold nugget, 47K Patch prospect

Table 1. LA-ICP-MS data for main elements (above detection limit) in three traverses for sample GSWA 201986: gold nugget, 47K Patch prospect

Ag (%)	Cu (ppm)	Hg (ppm)	Other elements (ppm) ¹ ²
8.1	651	213	Ca
7.1	583	283	Al, Ca
8.5	612	286	

NOTES: 1 See Table 2 for concentrations and detection limit
2 Results are only shown where standards are available for the element

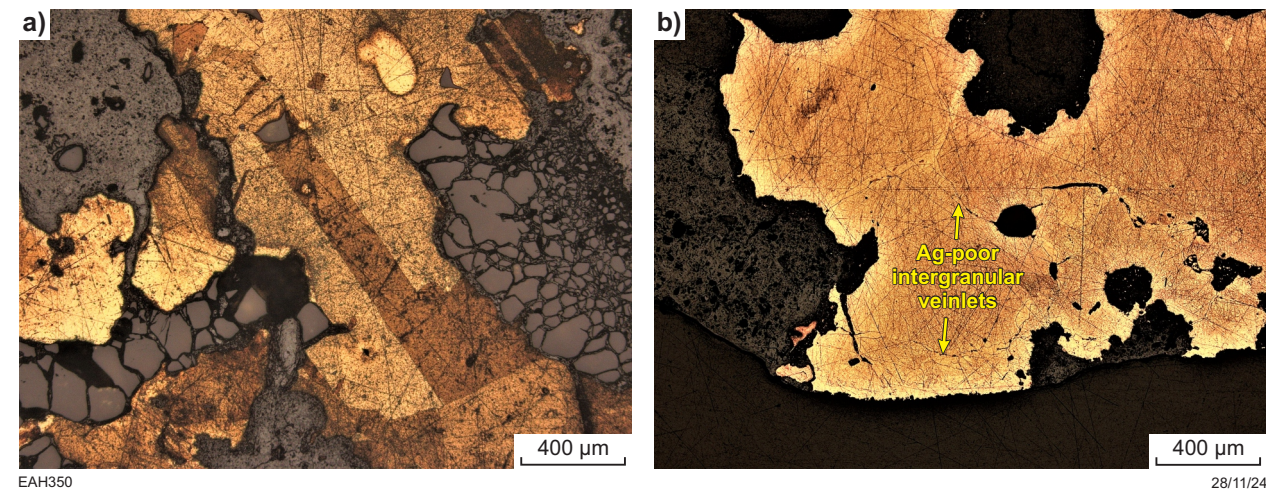


Figure 4. Reflected-light photomicrographs, after repolishing and acid etching, of parts of sample 201986: gold nugget, 47K Patch prospect

Table 2. LA-ICP-MS compositional data for sample GSWA 201986: gold nugget, 47K Patch prospect

Laser ablation track	Unit	⁷ Li	⁹ Be	¹¹ B	²³ Na	²⁵ Mg	²⁷ Al	²⁹ Si	⁴⁴ Ca	⁴⁵ Sc	⁴⁹ Ti	⁵¹ V	⁵³ Cr	⁵⁵ Mn	⁵⁷ Fe	⁵⁹ Co	⁶⁰ Ni	⁶⁵ Cu
1	cps					301	727		129	10	12	5		23	25		24	45415
2	cps			139		240	973		28	4	11					2	17	40613
3	cps		1			94	245				3		2		8		1	42668
1	ppm					2.93	0.98		16.8		0.21			0.07	1.04		0.35	651
2	ppm					2.34	1.31		3.72		0.20						0.25	583
3	ppm					0.92	0.33				0.06		0.05		0.37		0.03	612
DL*	ppm					3.3	1.3		2.6		1.5		1.7	1.1	3.4		2.9	1.5
Laser ablation track	Unit	⁶⁶ Zn	⁶⁹ Ga	⁷² Ge	⁷⁵ As	⁸² Se	⁸⁵ Rb	⁸⁸ Sr	⁸⁹ Y	⁹⁰ Zr	⁹³ Nb	⁹⁸ Mo	¹⁰¹ Ru	¹⁰³ Rh	¹⁰⁸ Pd	¹⁰⁹ Ag	¹¹¹ Cd	¹¹⁵ In
1	cps	87	2	1			19	9		3	4	1				9633916	6	
2	cps	34		1			14	2			1	3	1		2	8534998	2	
3	cps	28		1					4	1	4					10177629	2	
1	ppm	2.20														80700		
2	ppm	0.88													0.04	71500		
3	ppm	0.73														85200		
DL*	ppm	5.3			2	3.1								1.5	1.8	2.4		
Laser ablation track	Unit	¹²⁰ Sn	¹²¹ Sb	¹²⁶ Te	¹³³ Cs	¹³⁸ Ba	¹³⁹ La	¹⁴⁰ Ce	¹⁴¹ Pr	¹⁴⁵ Nd	¹⁵¹ Eu	¹⁵⁷ Gd	¹⁵⁹ Tb	¹⁶² Dy	¹⁶⁵ Ho	¹⁶⁷ Er	¹⁶⁹ Tm	¹⁷² Yb
1	cps	72	6			7		4	2									
2	cps	40	1		3	2				1		2						
3	cps	37			1			3										
1	ppm	0.52	0.05															
2	ppm	0.29	0.02															
3	ppm	0.27																
DL*	ppm	1.6	2.8	5.6														
Laser ablation track	Unit	¹⁷⁵ Lu	¹⁷⁸ Hf	¹⁸¹ Ta	¹⁸² W	¹⁸⁵ Re	¹⁸⁹ Os	¹⁹³ Ir	¹⁹⁵ Pt	²⁰² Hg	²⁰⁵ Tl	²⁰⁸ Pb	²⁰⁹ Bi	²³² Th	²³⁸ U			
1	cps									76519			11					
2	cps									77186		6						
3	cps									57389		3						
1	ppm									213			0.07					
2	ppm									283		0.06						
3	ppm									286		0.03						
DL*	ppm								2.5	2.5		1.5	2.2					

NOTES: cps, count per second; ppm, parts per million; DL, detection limit

*Detection limits have been determined using AuRM Reference Gold Standards (London Bullion Market Association). Standards were analysed nine times each and an average 2σ (95% confidence Interval) Limit of Detection determined. Some results given in the text are quoted as values that are below the detection limit for these analytes. These values must be considered as "for information" only.

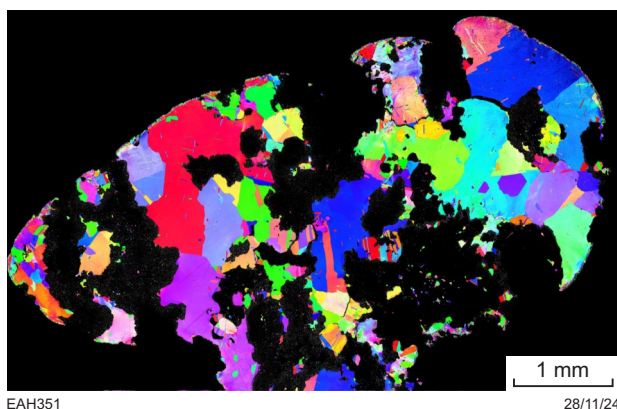


Figure 5. Electron back-scattered diffraction (EBSD) image of repolishing surface of gold grain extracted from sample 201986: gold nugget, 47K Patch prospect

Interpretation

The coherent gold in the nugget is polycrystalline and contains up to 8.5% Ag and moderate amounts of Cu and Hg, suggesting primary crystallization from hydrothermal fluids. Subsequent deformation, and hydrothermal and supergene alterations removed Ag by dissolution along intergranular veinlets, recrystallized the gold, and partly disaggregated the gold mass into several pieces, creating voids that subsequently filled with ferruginous clay and gold nanoparticles. Subsequent erosion and transport of the nugget in the surficial environment finely recrystallized the gold exposed at its outer rim, and entrapped Fe-oxide minerals and Fe–Al-rich film on its surface.

Acknowledgements

The authors gratefully acknowledge Michael Verrall (CSIRO) for his help with the SEM/EDS/EBSD operation and data interpretation, and samples preparation for EBSD analysis. We thank Professor John Watling for discussions to improve the LA-ICP-MS data interpretation.

References

- Artemis Resources Limited 2018, 225 Ounces of gold nuggets recovered from conglomerates (media release): Australian Securities Exchange (ASX), released 17 September 2018, 10p., <<https://wsecure.weblink.com.au/pdf/ARV/02022924.pdf>>.
- Geological Survey of Western Australia 2020, Northwest Pilbara, 2020: Geological Survey of Western Australia, Geological Information Series, data package (USB).
- Hancock, EA and Beardsmore, TJ 2020, Provenance fingerprinting of gold from the Kurnalpi Goldfield. Geological Survey of Western Australia Report 212, 21p.
- Hickman, AH 2016, Northwest Pilbara Craton: A record of 450 million years in the growth of Archean continental crust: Geological Survey of Western Australia, Report 160, 104p.
- Hickman, AH 2021, Bradley Basalt (A-WHb-b): Geological Survey of Western Australia, WA Geology Online, Explanatory Notes extract, viewed 04 May 2023, <www.demirs.wa.gov.au/ens>.
- Hickman, AH 2022, Yannerly Granite (A-STya-gfh): Geological Survey of Western Australia, WA Geology Online, Explanatory Notes extract, viewed 04 May 2023, <www.demirs.wa.gov.au/ens>.
- Murray, S 2009, LBMA certified reference materials. Gold project final update: The London Bullion Market Association, Alchemist, no. 55, p. 11–12.

Recommended reference for this publication

- Hancock, EA, Blay, OA and Beardsmore, TJ 2025, 201986: gold nugget, 47K Patch prospect; GSWA Mineralogy Record 20: Geological Survey of Western Australia, 5p.